Editors' Suggestion

Thermodynamic uncertainty relation in atomic-scale quantum conductors

Hava Meira Friedman [1], Bijay K. Agarwalla,[2] Ofir Shein-Lumbroso [3], Oren Tal [3] and Dvira Segal [1,4,*]

[1]*Chemical Physics Theory Group, Department of Chemistry, University of Toronto, 80 Saint George St., Toronto, Ontario, Canada M5S 3H6*

[2]*Department of Physics, Dr. Homi Bhabha Road, Indian Institute of Science Education and Research, Pune 411008, India*

[3]*Department of Chemical and Biological Physics, Weizmann Institute of Science, Rehovot 7610001, Israel*

[4]*Department of Physics, University of Toronto, Toronto, Ontario, Canada M5S 1A7*

(Received 31 January 2020; accepted 1 April 2020; published 15 May 2020)

The thermodynamic uncertainty relation (TUR), a trade-off relation between thermodynamic cost (entropy production) and precision (fluctuations), is expected to hold in nanoscale electronic conductors, when the electron transport process is quantum coherent and the transmission probability is constant (energy and voltage independent). We present measurements of the electron current and its noise in gold atomic-scale junctions and confirm the validity of the TUR for electron transport in realistic quantum coherent conductors. Furthermore, we show that it is beneficial to present the current and its noise as a TUR ratio to identify deviations from noninteracting-electron coherent dynamics.

DOI: 10.1103/PhysRevB.101.195423

I. INTRODUCTION

The thermodynamic uncertainty relation (TUR), a cost-precision trade-off relationship, has been of great interest recently in classical statistical physics. While it was originally conjectured for continuous-time, discrete-state Markov processes in a steady state [1], it was later proved based on the large deviation technique [2,3]. An incomplete list of studies on the TUR includes its generalizations to finite-time statistics [3–6], Langevin dynamics [4,7–10], periodic dynamics [11,12], and broken time-reversal-symmetry systems [13–15], as well as derivations of trade-off relations for heat engines [16]. Generalized versions of the TUR, which are based on the fundamental fluctuation symmetry for entropy production [17] were recently derived in Refs. [18,19]. Furthermore, a TUR bound for quantum systems in a nonequilibrium steady state was obtained in Ref. [20] using quantum information theoretic concepts.

For a two-terminal single-affinity system, the TUR connects the steady-state current $\langle j\rangle$, its variance $\langle\langle j^2\rangle\rangle = \langle j^2\rangle - \langle j\rangle^2$, and the average entropy production rate $\langle\sigma\rangle$ in a nonequilibrium process [1]:

$$\frac{\langle\langle j^2\rangle\rangle}{\langle j\rangle^2}\frac{\langle\sigma\rangle}{k_B} \geqslant 2. \tag{1}$$

Here, k_B is the Boltzmann constant. This relation, which was originally derived based on Markovian dynamics, reduces to an equality in linear response. Away from equilibrium, Eq. (1) describes the trade-off between precision and dissipation: A precise process with little noise is realized with high thermodynamic (entropic) cost. Systems that obey this inequality *satisfy the TUR*. TUR violations correspond to situations in which the left-hand side of Eq. (1) is smaller than 2. We refer to this special bound as the TUR—contrasting it to generalized TUR bounds—and we highlight that it is not universal and that it may be violated for certain processes [21].

Violations of the bound Eq. (1) were theoretically predicted in Refs. [21–23] for charge and energy transport problems in single and double quantum dot junctions in certain parameter regimes, when the transmission function was structured in the bias window. The first experimental interrogation of the bound Eq. (1) was recently reported in Ref. [24] by probing energy exchange between qubits—albeit in the *transient* regime. It was demonstrated in Ref. [24] that this bound could be violated by tuning the energy exchange parameters (qubit-qubit coupling), in line with theoretical predictions, and while satisfying the looser, generalized TUR bounds [18–20].

In what follows, we focus on the bound Eq. (1), rather than on its generalized forms [18,19] or the looser quantum bound [20], since it is expected to be valid for quantum transport junctions with a constant transmission probability [21]. Considering (single-affinity) steady-state charge transport under an applied bias voltage V, dissipation is given by Joule's heating, $\langle\sigma\rangle = \langle j\rangle\frac{V}{T}$, with T the temperature of the electronic system. The inequality Eq. (1) then simplifies to

$$\beta V\frac{\langle\langle j^2\rangle\rangle}{\langle j\rangle} \geqslant 2, \tag{2}$$

with $\beta = (k_BT)^{-1}$. For convenience, we introduce the combination $\mathcal{Q} \equiv \beta V\frac{\langle\langle j^2\rangle\rangle}{\langle j\rangle}$, which is a function of voltage and temperature. We refer to $\mathcal{Q}$ as the *TUR ratio*.

The TUR allows understanding of the trade-off between current fluctuations and entropy production. Furthermore, verifying or violating Eq. (2) provides insight into the underlying charge-transport statistics as was discussed in Ref. [21]. Atomic-scale junctions offer a rich playground for studying

*dvira.segal@utoronto.ca

steady-state quantum transport at the nanoscale [25]. It was pointed out in Ref. [21] that in junctions with a constant transmission probability, Eq. (2) should be valid. However, an experimental verification for this prediction is missing. Furthermore, beyond the fundamental interest in thermodynamical bounds, it might be useful to examine the behavior of the TUR ratio. We therefore ask here the following question: Does the measure $\mathcal{Q}$ reveal useful, additional information about the transport process beyond what is separately contained in the current and its fluctuations?

The objective of this paper is to study the TUR in charge-conducting atomic-scale junctions and use this compound measure to learn about charge-transport mechanisms in real systems. Different realizations of gold atomic-scale junctions depict distinct differential conductance traces [25]. Furthermore, corresponding shot-noise measurements display pronounced anomalous characteristics at high voltage [26–29]. Here, we confirm the validity of the TUR [Eq. (2)] in steady states using experimental data, in accord with theoretical predictions [21]. Furthermore, we argue that the TUR ratio can distill underlying transport mechanisms in atomic-scale junctions, which may be convoluted at the level of the current and its noise. The ratio $\mathcal{Q}$ begins at the equilibrium value of 2. We show that its linear behavior in voltage indicates the shared underlying quantum coherent dynamics. In contrast, a quadratic term in voltage distinguishes nonlinear contributions beyond the constant transmission limit.

Altogether, this study (i) validates and verifies the TUR in atomic-scale junctions and (ii) illustrates that the TUR can assist in diagnosing transport regimes. Yet more broadly, this study bridges a gap between quantum transport junctions [25] and stochastic thermodynamics [30,31], illustrating that thermodynamical bounds can be tested in nanoscale systems, in the quantum domain, down to the level of atomic-scale electronic conductors.

II. THEORY

A. TUR for normal shot noise

We consider nanoscale conductors in the quantum coherent limit with a constant transmission function (ohmic conductors), $\tau = \sum_i \tau_i$, collecting the contribution of independent transmission channels. The electrical current and its noise, under the chemical potential $\Delta\mu = \text{eV}$, are given by [25,32,33]

$$\begin{aligned}\langle j\rangle &= G_0 V \sum_i \tau_i,\\ \langle\langle j^2\rangle\rangle &= 2k_B T G_0 \sum_i \tau_i^2\\ &\quad + G_0 \sum_i \tau_i(1-\tau_i)\Delta\mu \coth\left(\frac{\Delta\mu}{2k_B T}\right).\end{aligned} \tag{3}$$

We identify the electrical conductance, $G = G_0 \sum_i \tau_i$, and the constant Fano factor $F = \sum_i \tau_i(1-\tau_i)/\sum_i \tau_i$. $G_0 = 2e^2/h$ is the quantum of conductance. Note that the zero-frequency spectral density of the noise, commonly denoted by $S(\omega = 0)$, is defined a factor of 2 greater than the second cumulant of the noise. The expression for the current noise combines the (zero voltage) thermal noise and the (zero temperature) shot noise. From these expressions, we prepare the TUR ratio:

$$\mathcal{Q} = 2 + \frac{\sum_i \tau_i(1-\tau_i)}{\sum_i \tau_i}\left[\frac{\Delta\mu}{k_B T}\coth\frac{\Delta\mu}{2k_B T} - 2\right]. \tag{4}$$

Since $x\coth x \geqslant 1$, the bound Eq. (2) is satisfied in the constant transmission limit, independent of voltage and temperature. In the high bias limit, $|\Delta\mu| \gg k_B T$, this relation reduces to

$$\mathcal{Q} = 2 + F\beta|\Delta\mu|. \tag{5}$$

Note that in this limit the current noise is $\langle\langle j^2\rangle\rangle = e|\langle j\rangle|F$, which is the quantum shot noise with the suppression factor F. In contrast, in the limit of very low voltage, we expand Eqs. (3) and get

$$\mathcal{Q} = 2 + \frac{(\beta\Delta\mu)^2}{6}F + \mathcal{O}((\Delta\mu)^4) + \cdots. \tag{6}$$

To study the latter expansion, one would need to inspect the current and its noise close to equilibrium. For $T = 7$ K, $\beta \approx 1500\ (\text{eV})^{-1}$ and $|\beta V| < 1$ requires scanning the noise for fine bias voltage $V < 1$ mV. In the experiments reported below, the voltage was scanned between 10 and 1000 mV, focusing on the examination of Eq. (5).

Comparing Eqs. (3) to Eq. (4), we note that these expressions are closely related. However, we argue that the TUR ratio, Eq. (4), provides a beneficial representation of the scaled noise since (i) its development from the equilibrium value of 2 to the high voltage regime can be clearly observed and (ii) it brings the data together onto a universal curve. In Sec. III we demonstrate these points on measured data.

B. TUR for anomalous shot noise

Measurements of shot noise in Au atomic-scale contacts reveal anomalous (nonlinear) characteristics at high voltage [26–29]. These observations were interpreted in Ref. [29] based on a coherent quantum transport model with two elements: The transmission function for electrons was assumed to be energy dependent and the voltage drop on the electrodes was allowed to be asymmetric.

For the Au atomic-scale junctions analyzed in this work, $G \approx 1G_0$, and it is therefore sufficient to consider two channels [25,29]: a primary channel, which is almost fully open, and a secondary channel with a low transmission probability. We model the transmission function of the dominant channel by the low order (linear) Taylor expansion $\tau_1(\epsilon) = \tau_1 + \tau_1'(\mu)(\epsilon - \mu)$, where τ_1 is the constant value of the transmission function at the Fermi energy and $\tau_1'(\mu)$ is the derivative of this function, evaluated at the Fermi energy. The contribution of the secondary channel is minor and for its transmission function we use the constant approximation, $\tau_2(\epsilon) \sim \tau_2 \ll \tau_1$. The partition of the bias voltage is quantified by the parameter α, with $\mu_L = \mu + \alpha\Delta\mu$ and $\mu_R = \mu - (1-\alpha)\Delta\mu$; $0 \leqslant \alpha \leqslant 1$; the bias voltage is symmetrically divided at the electrodes when $\alpha = 1/2$. It should be highlighted that the linear approximation for the transmission function describes only a certain class of measurements, while other atomic-scale junctions display more complicated trends [29].

The determinant for the energy- (and possibly voltage) dependent transmission function in Au atomic-scale junc-

tions could be quantum interference of electron waves with randomly placed defects in the metal contacts [28] or weak electron-phonon coupling effects [34]; our analysis does not presume the root for the functional form of $\tau(\epsilon)$.

The origin of the bias voltage asymmetry could be structural differences in the contact region at the left and right sides, such as different atomic configurations. Given such a microscopic spatial asymmetry, the mean-field parameter α emerges due to underlying many-body electron interaction effects, that is, the response of electrons in the junction to the applied electric field. While α is attained here as a fitting parameter for the differential conductance and noise, it could be resolved computationally based on atomistic-electronic structure calculations: Given a particular atomic configuration of the junction and with a certain applied bias voltage, one needs to perform self-consistent electronic structure and charge-transport calculations to determine the electron density in the junction and the corresponding potential drop across the junction.

Based on these ingredients, an energy-dependent transmission function and voltage drop asymmetry, expressions for the current (divided here already by voltage) and its noise were derived in Ref. [29],

$$\begin{aligned}\frac{\langle j\rangle}{V} &= G_0\sum_i \tau_i + G_0\tau_1'(\mu)(\alpha-1/2)\Delta\mu,\\ \langle\langle j^2\rangle\rangle &\approx 2k_BTG_0\sum_i\tau_i\\ &\quad + G_0k_BT\sum_i\tau_i(1-\tau_i)\left[\frac{\Delta\mu}{k_BT}\coth\left(\frac{\Delta\mu}{2k_BT}\right)-2\right]\\ &\quad + G_0(1-2\tau_1)\tau_1'(\mu)(\alpha-1/2)(\Delta\mu)^2. \qquad (7)\end{aligned}$$

The complete expression for the noise is included in Appendix A; here we already took the low-temperature limit $eV \gg k_BT$ and assumed that $|\tau'\Delta\mu| < 1$ and $\alpha \neq 1/2$. For simplicity, we define a combined nonlinear coefficient $\gamma \equiv (\alpha-1/2)\tau_1'(\mu)$, which has the physical dimension of inverse energy. This coefficient conjoins the two elements that are responsible for anomalous behavior: Many-body effects (phenomenologically captured by α) and an energy-dependent transmission probability.

We now write down the TUR ratio in the limit $eV \gg k_BT$ to the lowest order in $|\gamma\Delta\mu| < 1$, for the positive voltage branch:

$$\mathcal{Q} \approx 2 + \Delta\mu\beta F - \frac{2\gamma\Delta\mu}{\sum_i\tau_i} - \frac{\gamma\beta(\Delta\mu)^2}{\sum_i\tau_i}[F+(2\tau_1-1)]. \qquad (8)$$

We can simplify this expression by noting that in our experiments (see Sec. III) $\beta F \gg |\gamma|$ and that $\tau_2 \ll \tau_1$. We get

$$\frac{F+(2\tau_1-1)}{\sum_i\tau_i} = 1 - \frac{2\tau_2^2}{(\tau_1+\tau_2)^2} \approx 1, \qquad (9)$$

which simplifies Eq. (8) to

$$\mathcal{Q} \approx 2 + \Delta\mu\beta F - \gamma\beta(\Delta\mu)^2. \qquad (10)$$

This result is remarkable since the second, nonlinear term in voltage distills the nonlinear contribution γ. Since γ could be positive or negative, the TUR ratio may show either a suppression or an enhancement from the linear normal shot-noise term. Further, $\gamma\Delta\mu$ could be comparable to the constant Fano factor F, therefore the contribution of the quadratic term could be substantial. In fact, the TUR could be violated at high voltage once $F < \gamma\Delta\mu$.

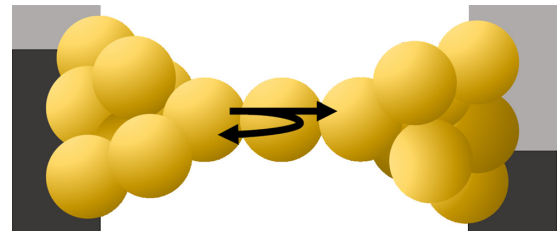

FIG. 1. An illustration of a gold atomic-scale junction realized with the break junction technique. At high bias voltage and zero temperature, electron current is unidirectional, with the transmitted and reflected components illustrated by arrows. The dark (light) regions at the left and right sides represent electron occupation (empty states). The atomic configuration at the junction varies, and the junction is not necessarily spatially symmetric. As a result, the applied voltage may be partitioned unevenly across the atomic-scale junction, quantified by the parameter α.

Altogether, we argue that presenting the noise as a TUR ratio is beneficial for elucidating transport processes. According to Eq. (10): (i) The constant term, 2, represents the equilibrium value. (ii) The linear term in voltage describes quantum suppressed-Poissonian dynamics and it identifies the corresponding Fano factor. This term emerges from a quantum coherent transport process with a constant transmission coefficient. (iii) The nonlinear term includes deviations from the constant transmission limit and it reflects the departure from the simple quantum coherent picture, with the involvement of many body effects (γ).

Equation (10) is valid at high voltage or, correspondingly, low temperature, $\Delta\mu \gg k_BT$. In Appendix A, we discuss the behavior of the TUR ratio for anomalous shot noise at high temperature.

III. ANALYSIS OF ATOMIC-SCALE GOLD JUNCTIONS

We test the theoretical expressions for the TUR ratio with measurements of the current and current fluctuations in Au atomic-scale junctions. The atomic junction and scattering processes are illustrated in Fig. 1. We use the mechanically controllable break junction technique at cryogenic conditions to form an ensemble of atomic-scale junctions [36]. By repeatedly breaking and reforming the junction, realizations with somewhat different atomic configurations are generated, supporting a range of conductance values of $G \approx 1G_0$. Differential conductance measurements are performed for each junction, as well as current-voltage traces and shot-noise measurements. More details about the experiment are included in Appendix B. For gold atomic-scale junctions, proximity-induced superconductivity measurements [37] and shot-noise analysis [38,39] suggest that a single channel dominates the conduction with a nearly perfect coupling to the metals [25].

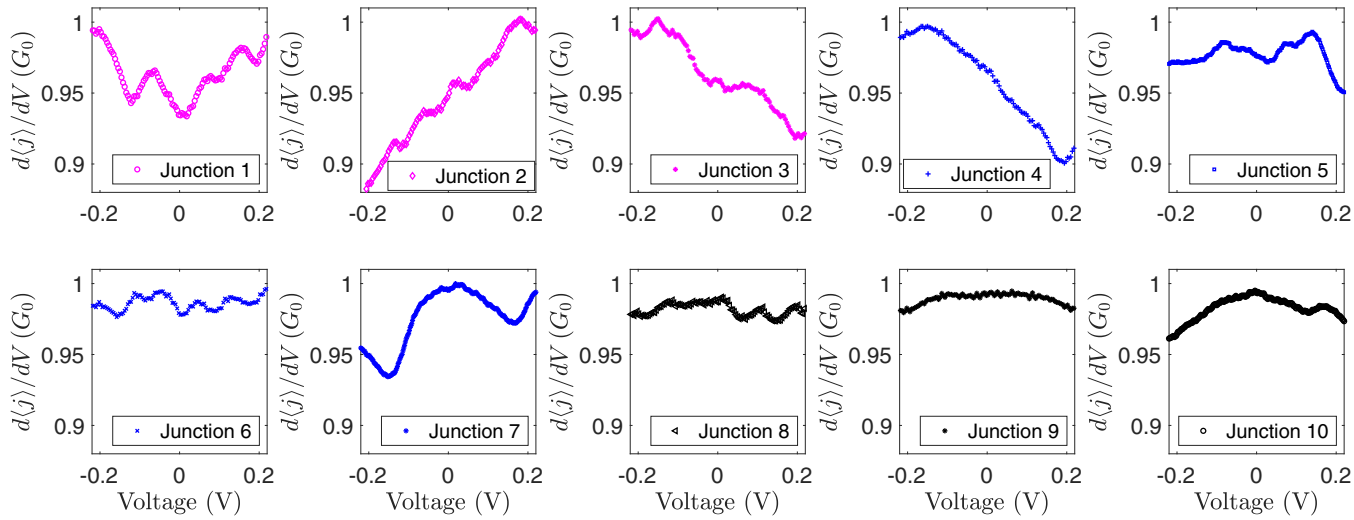

FIG. 2. Electrical conductance of 10 representative Au atomic-scale junctions formed using the mechanically controllable break-junction technique.

The data that we analyze: the differential conductance, current-voltage characteristics, and the shot noise for different atomic-scale junctions is shown in Figs. 2 and 3. Based on Fig. 3, we classify three regimes in the current noise: (i) The close-to-equilibrium or the low-voltage regime. In this case, eV is lesser or equal to the thermal energy and the thermal noise is prominent; if $T < 10$ K, $V < 5$ mV. The TUR in this regime [see Eq. (6) and Appendix A] is not probed in our work. (ii) Normal shot noise regime, 10 mV $< V \lesssim 75$ mV. In this region the current noise follows the standard-normal shot noise expression, and it is linear in voltage. (iii) Anomalous shot noise regime, around $V > 75$ mV. In this region the shot noise displays anomalous trends as it is no longer linear in voltage.

We extract the zero-voltage electrical conductance, $G = G_0 \sum_i \tau_i$, from the differential conductance at zero voltage. The electronic temperature is measured from the equilibrium noise $\langle\langle j^2\rangle\rangle = 2k_BTG$ and is in the range of $T = 5 - 10$ K (see also Appendix B). The constant Fano factor F is obtained by fitting the shot noise at low voltage (typically, $V < 20$ mV)

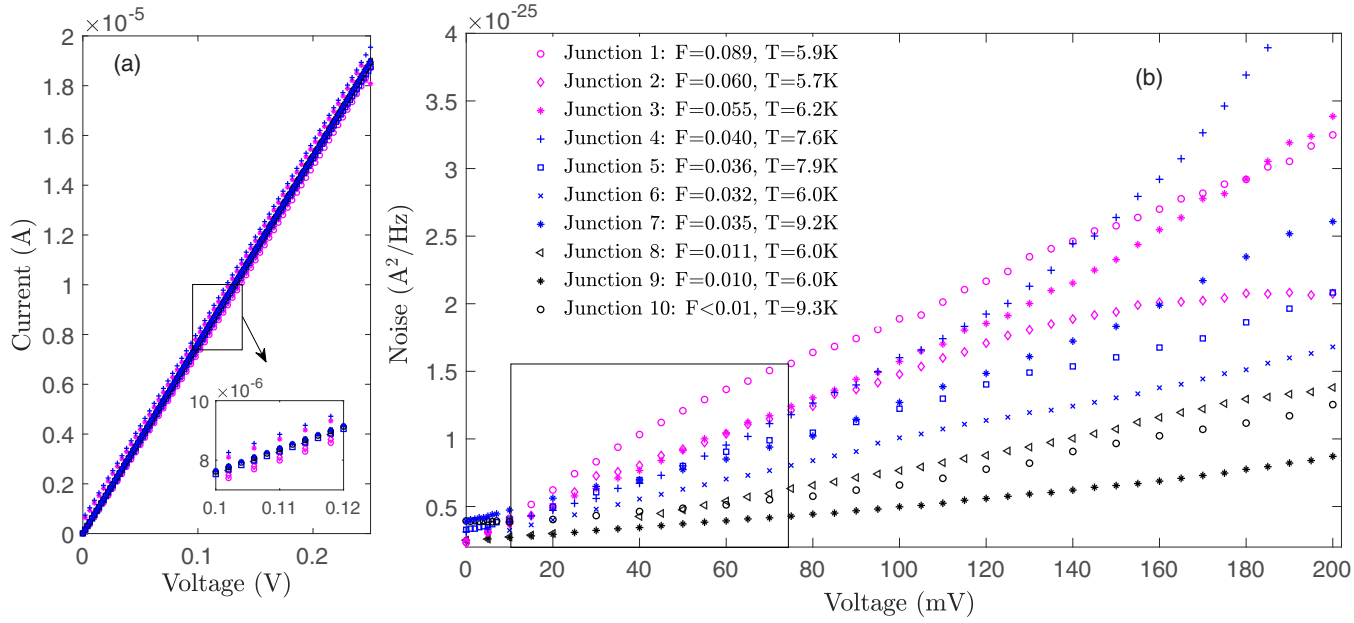

FIG. 3. (a) Current as a function of voltage and (b) its noise for each of the ten atomic-scale junctions of Fig. 2. The temperature (extracted from the equilibrium noise) and the constant Fano factor (obtained from the low-voltage noise) are presented in the legend. Depending on the specific region used for the calculation of the constant Fano factor, its value may vary by up to ±0.01 units. Values reported here were used below in Figs. 4 and 5 for further analysis. The noise is approximately linear in bias voltage for most junctions between 10 mV $< V <$ 75 mV, indicated by the region enclosed in a rectangle. For junction 10, the current noise does not display a normal shot-noise region, resulting in an undetermined (very small) Fano factor.

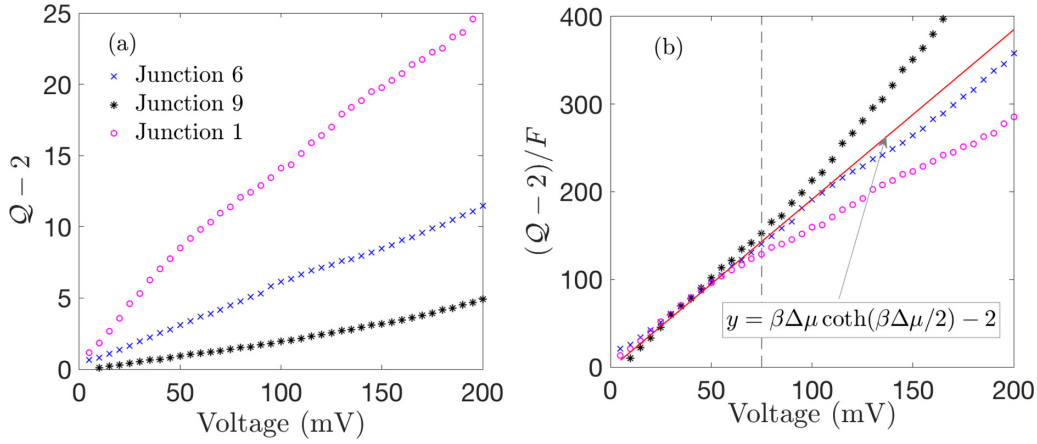

FIG. 4. (a) TUR ratio as a function of voltage for junctions with approximately a constant transmission function (junctions 6 and 9), as well as for junction 1, which shows an energy-dependent transmission function. (b) By plotting the data as $(\mathcal{Q}-2)/F$, the different curves collapse onto the universal function Eq. (4) before the dashed line, which marks the bias voltage 75 mV, beyond which deviations from the universal function show. The temperature, calculated from the equilibrium noise, is $T = 6.0$ K. $G = G_0 \sum \tau_i$ was obtained from the zero-voltage differential conductance. The constant Fano factor was deduced from the normal shot-noise regime, based on the behavior of the differential conductance and the noise. Not all voltage points in the noise trace were measured in the electrical current. However, since the current is highly linear in voltage, we performed a linear interpolation for the current-voltage curve and added the few missing points in between; we only interpolate for voltages higher than 10 mV.

to Eqs. (3) and dividing by the zero-voltage electrical conductance.

In Fig. 2, we display the differential conductance of ten representative junctions. While in some cases, the differential conductance is about constant with voltage, other junctions explicate a more significant variability of $d\langle j\rangle/dV$ with voltage, indicating deviations from Eqs. (3). We use different colors for different junctions roughly grouped according to their constant Fano factor. In Fig. 3(a), we display the currents for these ten junctions, which are nearly ohmic throughout. We further present the current noise in Fig. 3(b), which largely deviates from a linear behavior beyond $V \sim 75$ mV [29]. Recall that $\langle\langle j^2\rangle\rangle \propto |V|$ for ohmic conductors. Deviations from this trend are referred to as anomalous shot noise. This effect was the focus of Ref. [29].

To test Eq. (4), we select junctions 6 and 9 that display approximately a constant differential conductance (thus a constant transmission function), see Fig. 2 (we exclude junction 8 since its noise measurements were missing values in the normal shot-noise voltage regime). To contrast it, we also analyze junction 1 for which the differential conductance varies more substantially with voltage. While the temperature was similar for the three junctions ($T = 6.0 \pm 0.1$ K), the Fano factor was quite distinct, varying between 0.1 to 0.01.

We present the TUR ratio (after subtracting the equilibrium value), $\mathcal{Q}-2$ of the three junctions in Fig. 4(a). As expected, $\mathcal{Q} \geqslant 2$ throughout, Furthermore, by plotting the ratio $(\mathcal{Q}-2)/F$ in Fig. 4(b), we demonstrate that the measurements collapse on the universal function $\beta V \coth(\beta V/2) - 2$ up to around 75 mV for junctions 6 and 9. In fact, when $T \sim 6$ K [$\beta \sim 2000$ 1/(eV)], $|\coth \beta\Delta\mu/2| \approx 1$ beyond 5 mV, thus arriving at Eq. (5) with $(\mathcal{Q}-2)/F \approx \beta|\Delta\mu|$. The fact that the data agrees with Eq. (4) is not surprising, since F was extracted from the noise formula Eqs. (3). However, it is advantageous to present the data in this manner: The combination $(\mathcal{Q}-2)/F$ illustrates the common quantum coherent transport mechanism underlying the shot noise in these junctions for $V \lesssim 75$ mV.

We test Eq. (10), which describes deviations from the universal form by studying junctions 2 and 3. In these two cases, the differential conductance approximately follows a linear line—corresponding to the theoretical model behind Eqs. (7). Junction 4, which was analyzed in Ref. [29] suffers from more significant $1/f$ noise contribution and we therefore do not include it.

The slope of the differential conductance provides the coefficient 2γ, which is adopted in Eq. (10) to calculate the TUR ratio. Results are displayed in Fig. 5. The TUR ratio agrees with the constant transmission expression Eq. (4) up to $\approx$75 mV. However, as we increase the voltage, the nonlinear expression Eq. (10) provides a better description of the curved TUR function with the quadratic coefficient $\beta\gamma$. We retrieve $\gamma \sim 0.13$ $(\text{eV})^{-1}$ for junction 2. Given that $F = 0.06$ for this junction, the TUR could be violated at high voltage, $V > 0.6$ V. However, at this bias voltage, one would need to consider higher order $\gamma\Delta\mu$ terms in the expansion Eq. (10). For junction 3, we obtain $\gamma \sim -0.095$ $(\text{eV})^{-1}$, indicating the enhancement of the shot noise relative to the normal shot noise regime. The lowest-voltage TUR ratio for junction 3 seemingly violates the TUR. However, this point suffers from large relative error (since both the current and the noise are small), and we cannot draw conclusions based on this single observation. Careful measurements of the current and its noise at low voltage, $V < 10$ mV, would allow the analysis of the TUR close to equilibrium, as discussed in Appendix A.

Inelastic electron-phonon scattering processes give rise to nonlinear electronic noise in nanojunctions. Understanding these features is nontrivial, with ongoing research work aiming to resolve it in atomic and molecular junctions, see, e.g., Refs. [35,40–43]. Particularly, for Au point contacts, theoretical and experimental studies identified signatures of phonon activation with a distinct kink feature at the threshold voltage

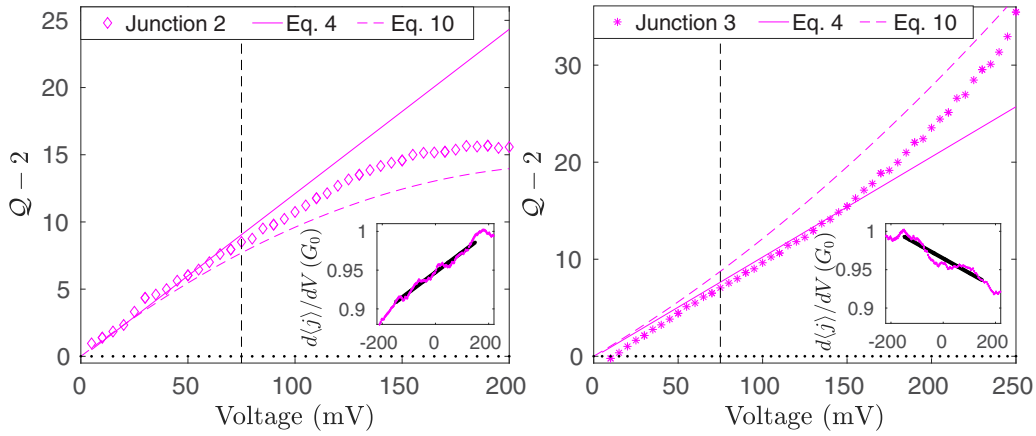

FIG. 5. TUR ratio in junctions 2 and 3 for which the differential conductance (inset), and therefore the transmission function can be approximated by a linear function. Measurements are compared to (full line) the constant transmission TUR, Eq. (4) and to the (dashed line) nonlinear expression, Eq. (10). Vertical lines at 75 mV mark the onset of the anomalous regime. The insets display the differential conductances for the two junctions, with a linear fit (dark full line) performed around zero voltage yielding the nonlinear coefficients (a) $\gamma = 0.129$ 1/eV and (b) $\gamma = -0.095$ 1/eV.

for vibration-mode excitation in Au, appearing around 15 to 25 mV [44–47]. In contrast, the current-noise displayed in Fig. 3 shows deviations from the linear shot-noise expression at higher bias, typically above 75 mV (see corresponding measurements reported in Ref. [28]). As discussed in detail in Ref. [29], the anomalous shot noise that we observe cannot be simply associated with phonon activation, given the behavior of the differential conductance and the range of voltage where these nonlinear features appear. Nevertheless, there are two points to be emphasized: (i) The *measured* charge current and electronic noise consist of (to some extent) electron-phonon effects yet, regardless, the main message of this work is that the TUR is satisfied in the normal and anomalous regimes. (ii) Our simplified *theoretical* treatment is based on the approximation of noninteracting electrons with elastic scatterings, albeit with many-body effects incorporated at a mean-field level. The α parameter accounts for the response of electrons in the junction to the applied voltage. The energy-dependent transmission function, which we do not specify, may enclose electron-vibration effects, e.g., with renormalized parameters [34]. A rigorous theoretical study of the status of the TUR under electron-phonon effects is left for future work.

IV. CONCLUSIONS

Cost-precision entropy-fluctuation trade-off relationships are fundamental to understanding nonequilibrium processes. In this paper, we focused on steady-state charge transport in atomic-scale junctions, a process which is essentially quantum coherent. Based on experimental data and theoretical derivations, we show that the TUR Eq. (1) is satisfied in this system, even when the noninteracting electron picture is corrected to include many-body effects (in a mean-field form). The generalized quantum TUR [20] is factor of 2 looser than this bound and is obviously satisfied in our system. Our paper illustrates that the TUR bound is advantageous for exploring the fundamentals of transport processes: The TUR ratio is developed from the equilibrium value and it therefore identifies far-from-equilibrium effects. Indeed, organizing the current noise as a TUR ratio is beneficial to understanding the charge-transport problem. This is clearly observed by the evolution of the noise from the linear-universal behavior at intermediate voltage to the anomalous regime at high voltage.

More broadly, our paper illustrates that atomic-scale junctions offer a rich test bed for studying theoretical results in stochastic thermodynamics-while extending these predictions to the quantum domain. As such, our combined theoretical-experimental analysis presents a step into consolidating the quantum transport and statistical thermodynamics research endeavors.

The TUR for charge transport in a steady state, Eq. (2), can be violated once the transmission function is structured with sharp resonances of width smaller than the thermal energy [21]. This situation might be realized in molecular junctions at room temperature and at low voltage. Specifically, quantum dot structures offer a rich playground for studying the suppression of electronic noise in nanodevices. Experiments that directly probe the behavior of high-order moments of the current [48–50] could be used to examine thermodynamical bounds [21,23]. Future work will be focused on the behavior of the current noise and the associated TUR in many-body systems such as transport junctions with pronounced electron-vibration coupling.

ACKNOWLEDGMENTS

D.S. acknowledges the Natural Sciences and Engineering Research Council (NSERC) of Canada Discovery Grant and the Canada Research Chairs Program. The work of H.M.F. was supported by the NSERC Postgraduate Scholarships-Doctoral program. O.T. appreciates the support of the Harold Perlman family and acknowledges funding by a research grant from Dana and Yossie Hollander, the Israel Science Foundation (Grant No. 1089/15), the Minerva Foundation (Grant No. 120865), and the European Research Council (Grant No. 864008).

APPENDIX A: EXPANSION OF THE TUR RATIO CLOSE TO EQUILIBRIUM

Equations (5) and (10), which we used to explain experimental data, were derived in the limit of high bias voltage, $eV \gg k_BT$. Here we study the complementary limit of high temperature (or low voltage) and discuss the possible violation of the TUR in this regime.

The electric current and its noise can be formally expanded in orders of the applied bias voltage as

$$\langle j\rangle = G_1V + \frac{1}{2!}G_2V^2 + \frac{1}{3!}G_3V^3 + ...$$
$$\langle\langle j^2\rangle\rangle = S_0 + S_1V + \frac{1}{2!}S_2V^2 + \frac{1}{3!}S_3V^3 + ... \quad \text{(A1)}$$

Here, G_1 is the linear conductance, G_2, G_3,... are the nonlinear coefficients in the current-voltage expansion. Similarly, S_0 is the equilibrium (Johnson Nyquist) noise, and S_1, S_2, are the nonequilibrium noise terms. We substitute these expansions into Eq. (2) and get [21]

$$\beta V\frac{\langle\langle j^2\rangle\rangle}{\langle j\rangle} = \frac{\beta}{G_1}S_0 + \frac{\beta V}{G_1}\Big[S_1 - \frac{S_0\,G_2}{2\,G_1}\Big] + \frac{\beta V^2}{G_1} \times\Big[\frac{S_2}{2} - \frac{S_0G_3}{6G_1} + \frac{S_0G_2^2}{4G_1^2} - \frac{S_1G_2}{2G_1}\Big] + \mathcal{O}(V^3) + \cdots \quad \text{(A2)}$$

We make use of the fluctuation-dissipation (Green-Kubo) relation, $S_0 = 2k_BTG_1$, and the first of the Saito-Utsumi relationships [51], $S_1 = k_BTG_2$, both resulting from the fluctuation relation [17], and reduce Eq. (A2) to

$$\beta V\frac{\langle\langle j^2\rangle\rangle}{\langle j\rangle} = 2 + \frac{V^2}{3S_0}[3S_2 - 2k_BTG_3] + \mathcal{O}(V^3) + \cdots. \quad \text{(A3)}$$

We now introduce the expansion of the TUR ratio around equilibrium:

$$\mathcal{Q} = 2 + Q_2(\beta V)^2 + Q_3(\beta V)^3 + \cdots. \quad \text{(A4)}$$

Here, Q_2, Q_3,... are coefficients of the TUR ratio, and they depend on internal parameters and temperature. Note that Q_1 is missing in this expansion [21]. A negative Q_2 identifies TUR violation in the second order of voltage.

We now specify this analysis to the gold atomic-scale junctions with $G \sim 1G_0$, as described in Sec. III and in Ref. [29]. To model quantum coherent transport in Au junctions, we assume: (i) The transmission function, which describes the probability for electrons to cross the junction, is linear in energy. (ii) The bias voltage is divided asymmetrically at the contacts, quantified by the parameter α. (iii) Two channels contribute to the transmission, a dominant one which is almost fully open and a secondary channel with a small transmission coefficient $\tau_2 \ll \tau_1$. (iv) We take into account the variation of the transmission function with energy for the dominant channel only. Using this setup, the charge current is given by [29]

$$\langle j\rangle = \frac{2e}{h}\sum_{i=1,2}\tau_i\Delta\mu + \frac{2e}{h}\tau_1'(\mu)\Big(\alpha - \frac{1}{2}\Big)(\Delta\mu)^2. \quad \text{(A5)}$$

The linear conductance and the nonlinear coefficients can be collected as

$$G_1 = G_0\sum_i\tau_i, \quad G_2 = G_0\tau_1'(\mu)(\alpha - 1/2)(2e),$$
$$G_3 = 0. \quad \text{(A6)}$$

The shot noise is given by [29]

$$\begin{aligned}\langle\langle j^2\rangle\rangle/G_0 = {}& 2k_BT\sum_i\tau_i^2 + \sum_i\tau_i(1-\tau_i)\Delta\mu\coth\Big(\frac{\Delta\mu}{2k_BT}\Big)\\ &+ 2k_BT\tau_1\tau_1'(\mu)\Delta\mu(2\alpha - 1)\\ &+ 2k_BT[\tau_1'(\mu)]^2\frac{\pi^2k_B^2T^2}{3} + k_BT[\tau_1'(\mu)]^2\\ &\times[\alpha^2(\Delta\mu)^2 + (1-\alpha)^2(\Delta\mu)^2]\\ &+ \coth\Big(\frac{\Delta\mu}{2k_BT}\Big)(1-2\tau_1)\tau_1'(\mu)\Big(\alpha - \frac{1}{2}\Big)(\Delta\mu)^2\\ &- \coth\Big(\frac{\Delta\mu}{2k_BT}\Big)[\tau_1'(\mu)]^2\Big[\Delta\mu\frac{\pi^2k_B^2T^2}{3}\\ &+ \frac{1}{12}(\Delta\mu)^3 + \Big(\alpha - \frac{1}{2}\Big)^2(\Delta\mu)^3\Big], \end{aligned} \quad \text{(A7)}$$

with the first three coefficients (A1),

$$S_0 = 2k_BTG_0\sum_i\tau_i, \quad S_1 = k_BTG_0(\alpha - 1/2)\tau_1'(\mu)(2e),$$
$$S_2 = G_0e^2\frac{\sum_i\tau_i(1-\tau_i)}{3k_BT} - k_BTe^2G_0\frac{(\pi^2-6)(\tau_1')^2}{9}. \quad \text{(A8)}$$

We can now verify the fluctuation-dissipation relation, $S_0 = 2k_BTG_1$, as well as the first of the Saito-Utsumi relations, $S_1 = k_BTG_2$. Indeed, though α (phenomenologically) builds on many-body effects, we can still write down the Levitov-Lesovik formula for the cumulant generating function and show that it satisfies the exchange steady-state fluctuation symmetry [17]. Since $G_3 = 0$, the series for the TUR ratio, Eq. (A4), reduces to

$$\beta V\frac{\langle\langle j^2\rangle\rangle}{\langle j\rangle} = 2 + V^2\frac{S_2}{S_0} + \mathcal{O}(V^3) + \cdots. \quad \text{(A9)}$$

Substituting S_0 and S_2, we get

$$\beta V\frac{\langle\langle j^2\rangle\rangle}{\langle j\rangle} = 2 + \frac{(\text{eV})^2}{6}\Big[\beta^2F - \frac{(\tau_1')^2(\pi^2-6)}{3\sum_i\tau_i}\Big] + \mathcal{O}(V^3). \quad \text{(A10)}$$

This expansion is valid only close to equilibrium, and as such it is complementary to Eq. (8), which was derived at high voltage.

Based on Eq. (A10), can we observe violations of the TUR in atomic-scale junctions in the low-voltage regime? For Au atomic-scale junctions $\sum_i\tau_i \approx 1$, $F \sim 0.01 - 0.1$ and $\tau_1' < 0.1$ 1/(eV). Therefore, the TUR is satisfied even at high temperatures, $T = 1000$ K. However, in systems with

a small transmission coefficient, $\tau \ll 1$ (possibly molecular junctions), TUR violations could be expected at high temperature once $\tau < (\tau_1')^2(k_BT)^2$.

Altogether, the TUR is satisfied in atomic-scale junctions given that the transmission coefficient is constant (energy independent). Furthermore, as discussed in Ref. [21], while the single resonance-level model can only display very weak TUR violations at high temperature, double-dot models could break the TUR quite substantially depending on the intersite coupling and the metal-dots hybridization energy.

APPENDIX B: EXPERIMENTAL PROCEDURE

The experimental procedure was described in Ref. [29] and we repeat it here for completeness.

1. Formation of Au atomic junctions

Au atomic junctions are formed with the mechanically controllable break-junction technique in cryogenic temperature. A gold wire (99.99%, 0.1 mm diameter, Goodfellow) with a partial cut in its center is attached to a flexible and insulating substrate. This structure is placed in a vacuum chamber, pumped to 10^{-5} mbar and cooled to 4.2 K. The sample is then bent by a piezoelectric element. As a result, the constriction at the wire center can be reduced to a few-atom contact, down to a single-atom contact between the two wire segments. New atomic junctions are formed by repeated squeezing of the electrodes against each other, followed by stretching the reformed metallic contact. This procedure allows the characterization of an ensemble of atomic junctions with somewhat different atomic configurations.

2. Differential conductance

Differential conductance versus voltage measurements are conducted with a standard lock-in technique using a Stanford Research SR830 lock-in amplifier. A DC bias voltage signal from a National Instruments (NI) PXI-4461 DAQ card is modulated by an AC voltage produced by the lock-in amplifier (1 mV rms at about 3.33 kHz). The current across the sample is amplified by a current preamplifier (SR570) and sent back to the lock-in to extract the corresponding signal at the frequency of the applied AC modulation. Differential conductance measurements are performed twice, before and after each set of noise measurements. By comparing the two differential conductance results, we confirm that the atomic contact maintains its stability during noise measurements.

3. Shot Noise

To measure shot noise on atomic junctions, the sample is disconnected from the conductance-measurement circuit and connected to a dedicated circuit [36]. The sample is current-biased by a Yokogawa GS200 SC voltage source connected to the sample through two 0.5MΩ resistors located in proximity to the sample. The resulting voltage noise is amplified by a custom-made differential low-noise amplifier and analyzed via a NI PXI-5922 DAQ card, using a LabView implemented fast Fourier transform analysis. For each stable atomic junction, noise measurements are conducted at a set of different biases, where at each bias 3000 measurements of noise spectra are taken and averaged. The temperature presented in Fig. 3 is extracted from the measured thermal noise. This temperature analysis is validated based on an amplifier and setup calibration, as described in Ref. [36].

[1] A. C. Barato and U. Seifert, Thermodynamic Uncertainty Relation for Biomolecular Processes, Phys. Rev. Lett. **114**, 158101 (2015).

[2] T. R. Gingrich, J. M. Horowitz, N. Perunov, and J. L. England, Dissipation Bounds All Steady-State Current Fluctuations, Phys. Rev. Lett. **116**, 120601 (2016).

[3] J. M. Horowitz and T. R. Gingrich, Proof of the finite-time thermodynamic uncertainty relation for steady-state currents, Phys. Rev. E **96**, 020103(R) (2017).

[4] A. Dechant, Multidimensional thermodynamic uncertainty relations, J. Phys. A: Math. Theor. **52**, 035001 (2019).

[5] P. Pietzonka, F. Ritort, and U. Seifert, Finite-time generalization of the thermodynamic uncertainty relation, Phys. Rev. E **96**, 012101 (2017).

[6] S. Pigolotti, I. Neri, E. Roldán, and F. Jülicher, Generic Properties of Stochastic Entropy Production, Phys. Rev. Lett. **119**, 140604 (2017).

[7] T. R. Gingrich, G. M. Rotskoff and J. M Horowitz, Inferring dissipation from current fluctuations, J. Phys. A: Math. Theor. **50**, 184004 (2017).

[8] Y. Hasegawa and T. V. Vu, Uncertainty relations in stochastic processes: An information inequality approach, Phys. Rev. E **99**, 062126 (2019).

[9] D. Gupta and A. Maritan, Thermodynamic Uncertainty relations in a linear system, Eur. Phys. J. B **93**, 28 (2020).

[10] C. Hyeon and W. Hwang, Physical insight into the thermodynamic uncertainty relation using Brownian motion in tilted periodic potentials, Phys. Rev. E **96**, 012156 (2017).

[11] T. Koyuk, U. Seifert, and P. Pietzonka, A generalization of the thermodynamic uncertainty relation to periodically driven systems, J. Phys. A: Math. Theor. **52**, 02LT02 (2018).

[12] A. C. Barato, R. Chetrite, A. Faggionato, and D. Gabrielli, Bounds on current fluctuations in periodically driven systems, New J. Phys. **20**, 103023 (2018).

[13] H.-M. Chun, L. P. Fischer, and U. Seifert, Effect of a magnetic field on the thermodynamic uncertainty relation, Phys. Rev. E **99**, 042128 (2019).

[14] K. Brandner, T. Hanazato, and K. Saito, Thermodynamic Bounds on Precision in Ballistic Multiterminal Transport, Phys. Rev. Lett. **120**, 090601 (2018).

[15] K. Proesmans and J. M. Horowitz, Hysteretic thermodynamic uncertainty relation for systems with broken time-reversal symmetry, J. Stat. Mech. (2019) 054005.

[16] P. Pietzonka and U. Seifert, Universal Trade-Off Between Power, Efficiency, and Constancy in Steady-State Heat Engines, Phys. Rev. Lett. **120**, 190602 (2018)

[17] M. Esposito, U. Harbola, and S. Mukamel, Nonequilibrium fluctuations, fluctuation theorems, and counting statistics in quantum systems, Rev. Mod. Phys. **81**, 1665 (2009).

[18] Y. Hasegawa and T. Van Vu, Fluctuation Theorem Uncertainty Relation, Phys. Rev. Lett. **123**, 110602 (2019).

[19] A. M. Timpanaro, G. Guarnieri, J. Goold, and G. T. Landi, Thermodynamic Uncertainty Relations from Exchange Fluctuation Theorems, Phys. Rev. Lett. **123**, 090604 (2019).

[20] G. Guarnieri, G. T. Landi, S. R. Clark, J. Goold, Thermodynamics of precision in quantum nonequilibrium steady states, Phys. Rev. Res. **1**, 033021 (2019).

[21] B. K. Agarwalla and D. Segal, Assessing the validity of the thermodynamic uncertainty relation in quantum systems, Phys. Rev. B **98**, 155438 (2018).

[22] S. Saryal, H. Friedman, D. Segal, and B. K. Agarwalla, Thermodynamic uncertainty relation in thermal transport, Phys. Rev. E **100**, 042101 (2019).

[23] J. Liu and D. Segal, Thermodynamic uncertainty relation in quantum thermoelectric junctions, Phys. Rev. E **99**, 062141 (2019).

[24] S. Pal, S. Saryal, D. Segal, S. Mahesh, and B. K. Agarwalla, Experimental study of the thermodynamic uncertainty relation, arXiv:1912.08391.

[25] J. C. Cuevas and E. Scheer, *Molecular Electronics: An Introduction to Theory and Experiment* (World Scientific, Singapore, 2010).

[26] R. Chen, P. J. Wheeler, M. Di Ventra, and D. Natelson, Enhanced noise at high bias in atomic-scale break junctions, Sci. Rep. **4**, 4221 (2015).

[27] L. A. Stevens, P. Zolotavin, R. Chen, and D. Natelson, Current noise enhancement: Channel mixing and possible nonequilibrium phonon backaction in atomic scale Au junctions, J. Phys.: Condens. Matter **28**, 495303 (2016).

[28] S. Tewari and J. van Ruitenbeek, Anomalous nonlinear shot noise at high voltage bias, Nano Lett. **18**, 5217 (2018).

[29] A. Mu, O. Shein-Lumbroso, O. Tal and D. Segal, Origin of the anomalous electronic shot noise in atomic-scale junctions, J. Phys. Chem. C **123**, 6099 (2019).

[30] U. Seifert, From stochastic thermodynamics to thermodynamic inference, Ann. Rev. Condens. Mater. Phys. **10**, 171 (2019).

[31] R. Marsland III and J. England, Limits of predictions in thermodynamic systems: A review, Rep. Prog. Phys. **81**, 016601 (2018).

[32] Ya. M. Blanter and M. Buttiker, Shot noise in mesoscopic conductors, Phys. Rep. **336**, 1 (2000).

[33] *Quantum Noise in Mesoscopic Physics*, edited by Yu. V. Nazarov, NATO Advanced Research Workshop (Springer, New York, 2003).

[34] Weak electron-phonon couplings lead to the renormalization of the elastic transmission channel, as well as the opening of inelastic channels. Considering weak electron-phonon interactions and in the limit of large hybridization, which is relevant for our study, it can be shown that the current and its noise follow Landauer-like expressions as used here, albeit with modified, *energy-dependent* transmission functions [35].

[35] M. Galperin, A. Nitzan, and M. A. Ratner, Inelastic tunneling effects on noise properties of molecular junctions, Phys. Rev. B **74**, 075326 (2006).

[36] O. Shein Lumbroso, L. Simine, A. Nitzan, D. Segal and O. Tal, Electronic noise due to temperature difference in atomic-scale junctions, Nature **562**, 240 (2018).

[37] E. Scheer, W. Belzig, Y. Naveh, M. H. Devoret, D. Esteve, C. Urbina, Proximity Effect and Multiple Andreev Reflections in Gold Point Contacts, Phys. Rev. Lett. **86**, 284 (2001).

[38] R. Vardimon, M. Klionsky, and O. Tal, Experimental determination of conduction channels in atomic-scale conductors based on shot noise measurements, Phys. Rev. B **88**, 161404(R) (2013).

[39] R. Vardimon, T. Yelin, M. Klionsky, S. Sarkar, A. Biller, L. Kronik, O. Tal, Probing the orbital origin of conductance oscillations in atomic chains, Nano Lett. **14**, 2988 (2014).

[40] C. Schinabeck, R. Härtle, H. B. Weber, and M. Thoss, Current noise in single-molecule junctions induced by electronic-vibrational coupling, Phys. Rev. B **90**, 075409 (2014).

[41] B. K. Agarwalla, J.-H. Jiang, and D. Segal, Full counting statistics of vibrationally assisted electronic conduction: Transport and fluctuations of thermoelectric efficiency, Phys. Rev. B **92**, 245418 (2015).

[42] C. Schinabeck and M. Thoss, Hierarchical quantum master equation approach to current fluctuations in nonequilibrium charge transport through nanosystems, Phys. Rev. B **101**, 075422 (2020).

[43] F. Evers, R. Korytar, S. Tewari, and J. M. van Ruitenbeek, Advances and challenges in single-molecule electron transport, arXiv:1906.10449.

[44] M. Kumar, R. Avriller, A. L. Yeyati, and J. M. van Ruitenbeek, Detection of Vibration-Mode Scattering in Electronic Shot Noise, Phys. Rev. Lett. **108**, 146602 (2012).

[45] R. Avriller and T. Frederiksen, Inelastic shot noise characteristics of nanoscale junctions from first principles, Phys. Rev. B **86**, 155411 (2012).

[46] S. Kim, Inelastic current noise in nanoscale systems: Scattering theory analysis, Phys. Rev. B **89**, 035413 (2014).

[47] S. G. Bahoosh, M. A. Karimi, W. Belzig, E. Scheer, and F. Pauly, Influence of electron-vibration interactions on electronic current noise of atomic and molecular junctions, arXiv:1912.13496.

[48] S. Gustavsson, R. Leturcq, B. Simovič, R. Schleser, T. Ihn, P. Studerus, K. Ensslin, D. C. Driscoll, and A. C. Gossard, Counting Statistics of Single Electron Transport in a Quantum Dot, Phys. Rev. Lett. **96**, 076605 (2006).

[49] S. Gustavsson, R. Leturcq, B. Simovič, R. Schleser, P. Studerus, T. Ihn, K. Ensslin, D. C. Driscoll, and A. C. Gossard, Counting statistics and super-Poissonian noise in a quantum dot: Time-resolved measurements of electron transport, Phys. Rev. B **74**, 195305 (2006).

[50] N. Ubbelohde, C. Fricke, C. Flindt, F. Hohls and R. J. Haug, Measurement of finite-frequency current statistics in a single-electron transistor, Nat. Commun. **3**, 612 (2012).

[51] K. Saito and Y. Utsumi, Symmetry in full counting statistics, fluctuation theorem, and relations among nonlinear transport coefficients in the presence of a magnetic field, Phys. Rev. B **78**, 115429 (2008).